Title
TWO-MAGNON RESONANT RAMAN SCATTERING IN MnF2

Authors
Amer, Natal M.
Chiang, Tai-chang.
Shen, Y.R.

Publication Date
1975-03-01

Submitted to Physical Review Letters

LBL-3747
Preprint

TWO-MAGNON RESONANT RAMAN SCATTERING IN MnF_2

Nabil M. Amer, Tai-chang Chiang, and Y. R. Shen

March 1975

Prepared for the U. S. Atomic Energy Commission
under Contract W-7405-ENG-48

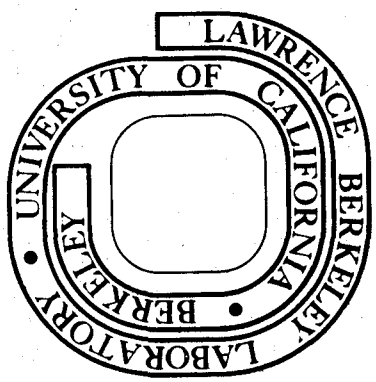

DISCLAIMER

Submitted to Physical Review Letters

LBL-3747
Preprint

UNIVERSITY OF CALIFORNIA

Lawrence Berkeley Laboratory
Berkeley, California

AEC Contract No. W-7405-eng-48

TWO-MAGNON RESONANT RAMAN SCATTERING IN MnF_2

Nabil M. Amer, Tai-chang Chiang, and Y. R. Shen

MARCH 1975

Two-Magnon Resonant Raman Scattering in MnF_2

Nabil M. Amer, Tai-chang Chiang, and Y. R. Shen
Department of Physics, University of California, and
Inorganic Materials Research Division,
Lawrence Berkeley Laboratory, Berkeley, California 94720

ABSTRACT

We have studied two-magnon resonant Raman scattering in MnF_2 around the magnon sidebands. The resonant scattering involves a different physical mechanism than the non-resonant case and leads to a number of new results. A simple theoretical description explains the experimental observations successfully.

Resonant Raman scattering (RRS) has so far been limited to semiconductors.[1] We report here the first investigation on RRS in a magnetically ordered crystal, e.g., MnF_2 in the antiferromagnetic phase. Because of space limitation, we shall discuss only RRS by two magnons in MnF_2 in some detail.

The magnon spectrum of the antiferromagnetic MnF_2 is well known.[2] The optical properties of MnF_2 has also been well studied, especially those involving magnons.[3-5] There is a set of sharp absorption lines around 18450 cm^{-1} (see Fig. 1) arising from transitions within the $^6A_{1g}(^6S) \rightarrow {}^4T_{1g}(^4G)$ manifold.[3] Lines e_1 and e_2 are due to creation of E_1 and E_2 excitons respectively via direct magnetic-dipole transitions while lines σ_1, π_1, and σ_2 are the corresponding magnon sidebands. In the luminescence spectrum,[5] direct and magnon-assisted recombinations of the E_1 excitons give rise to the e_{1L} and σ_{1L} (π_{1L}) luminescence lines respectively.

The Raman spectrum of MnF_2 has also been thoroughly studied.[6-8] It consists of four phonon modes and one two-magnon line. No one-magnon line has yet been observed. We are interested in the changes of the Raman and luminescence spectrum when the excitation scans through the absorption lines in Fig. 1.

Theoretically, the peak position and the cross-section of the two-magnon line for excitation near σ_1, π_1, and σ_2 lines can be obtained following, for example, Loudon's derivation.[4,6,7] The spin Hamiltonian is of the form (unless specified, we use the notations of Ref. 6)

$$H_s = \sum_{<i,j>} \sum_{\alpha,\beta} C_{ij}^{\alpha\beta} E_\ell^\alpha E_s^{\beta *} S_i^- S_j^+ \qquad (1)$$

where $C_{ij}^{\alpha\beta} = A_{ij}^{\alpha\beta} + B_{ij}^{\alpha\beta}$

$$A_{ij}^{\alpha\beta} = \sum_{\mu,\nu} \frac{\langle g_i\downarrow g_j\uparrow| \, er_\beta |g_i\downarrow \nu_j\uparrow\rangle\langle g_i\downarrow \nu_j\uparrow|V_{ex}|\mu_i\uparrow g_j\downarrow\rangle\langle\mu_i\uparrow g_j\downarrow|er_\alpha|g_i\uparrow g_j\downarrow\rangle}{(E_\nu-\hbar\omega_s)(E_\mu-\hbar\omega_\ell)}$$

+ 11 similar terms

$$B_{ij}^{\alpha\beta} \cong \sum_{\mu,\nu} \frac{\langle g_i\downarrow g_j\uparrow|er_\beta|\nu_i\downarrow g_j\uparrow\rangle\langle\nu_i\downarrow g_j\uparrow|V|e_i\downarrow g_j\uparrow\rangle\langle e_i\downarrow g_j\uparrow|V_{ex}|\mu_i\uparrow g_j\downarrow\rangle\langle\mu_i\uparrow g_j\downarrow|er_\alpha|g_i\uparrow g_j\downarrow\rangle}{(E_\nu-\hbar\omega_s)(E_\mu-\hbar\omega_\ell)\hbar(\omega_\ell-\omega_E-\omega_m+i\Gamma)}.$$

In the above equations, $\langle g_i|$ is the ground state of the ith Mn ion, $\langle\mu|$ and $\langle\nu|$ are the allowed excited states with energies E_μ and E_ν respectively, and $\langle e|$ is either the E_1 or the E_2 excitonic state with its energy denoted by $\hbar\omega_E$. The magnon frequency is ω_m. The quantities E_ℓ^α and E_s^β represent the α component of the exciting field and the β component of the scattered field respectively, and V and V_{ex} are respectively the direct and exchange terms of the Coulomb interaction. From Eq. (1) we find for the two-magnon Raman cross-section,

$$\frac{d\sigma_{\alpha\beta}}{d\omega_s} = \sum_{\vec{k}} \left| a_{\alpha\beta} + \frac{b_{\alpha\beta}}{\omega_\ell-\omega_E(\vec{k})-\omega_m(\vec{k})+i\Gamma}\right|^2 f_{\alpha\beta}(\vec{k}) \frac{\Gamma'}{|\omega_\ell-\omega_s-2\omega_m(\vec{k})+i\Gamma'|^2} \qquad (2)$$

where $a_{\alpha\beta}$ and $b_{\alpha\beta}$ are constant coefficients if we assume the matrix elements in Eq. (1) are constant and $f_{\alpha\beta}(\vec{k})$ is a function of $\vec{k}$. Since the $b_{\alpha\beta}$ term is obtained from higher-order perturbation than the $a_{\alpha\beta}$ term, the former should be negligible in comparison with the latter unless the excitation frequency is close to one of the magnon sidebands, i.e., $\omega_\ell \sim \omega_E + \omega_m(\vec{k})$. Near such a resonance, if we use the approximation $|x+i\Gamma|^{-2} \approx \pi\delta(x)/\Gamma$, we can write

$$d\sigma_{\alpha\beta}/d\omega_s \cong (d\sigma_{\alpha\beta}/d\omega_s)_{NR} + (d\sigma_{\alpha\beta}/d\omega_s)_R \tag{3}$$

with

$$(d\sigma_{\alpha\beta}/d\omega_s)_{NR} = (\pi|a_{\alpha\beta}|^2/\Gamma') \sum_{\vec{k}} f_{\alpha\beta}(\vec{k})\,\delta[\omega_\ell-\omega_s-2\omega_m(\vec{k})] \tag{3a}$$

$$(d\sigma_{\alpha\beta}/d\omega_s)_R = (\pi^2|b_{\alpha\beta}|^2/\Gamma\Gamma') \sum_{\vec{k}} f_{\alpha\beta}(\vec{k})\,\delta[\omega_\ell-\omega_E(\vec{k})-\omega_m(\vec{k})]\,\delta[\omega_\ell-\omega_s-2\omega_m(\vec{k})]. \tag{3b}$$

The total two-magnon Raman cross-section is then given by

$$\sigma_{\alpha\beta} = (\sigma_{\alpha\beta})_{NR} + (\sigma_{\alpha\beta})_R \tag{4}$$

where $(\sigma_{\alpha\beta})_R \propto [(d\sigma_{\alpha\beta}(\omega_\ell-\omega_s = 2\omega_\ell-2\omega_E)/d\omega_s]_{NR}$.
Equation (3b) shows that at resonance, if $(d\sigma_{\alpha\beta}/d\omega_s)_R > (d\sigma_{\alpha\beta}/d\omega_s)_{NR}$, the peak position of the two-magnon line is determined by

$$\omega_\ell-\omega_s = 2\omega_m(\vec{k}) = 2\omega_\ell-2\omega_E(\vec{k}). \tag{5}$$

The above results are easy to understand physically since the resonant part can be considered as due to a magnon-assisted absorption immediately followed by a magnon-assisted emission.

A cw dye laser with a linewidth of 0.2 cm^{-1} was used as the excitation source and the sample was immersed in superfluid He at 1.6°K. The luminescence spectrum was essentially identical to those reported in the literature but with less impurity lines, none in the range between 18340 and 18440 cm^{-1}, except the one (denoted by I in Fig. 2) overlapping with

the σ_{1L} line.[5]

Our results on resonance fluorescence (RF) and RRS by phonons in MnF_2 will be reported elsewhere. Here, we discuss only RRS by two magnons. We found that the two-magnon line showed a resonance enhancement at the magnon sidebands but not at the e_1 and e_2 exciton lines, just as we expected. Figure 2 shows a set of two-magnon Raman spectra at several different excitation frequencies around σ_1 and σ_2. It is seen that the two-magnon line (denoted by M) varies in frequency with ω_ℓ. Deep in resonance, the line is considerably sharper (limited by instrument resolution in Fig. 2). When ω_ℓ falls in the region where σ_1 and σ_2 overlap, two two-magnon lines show up, due to simultaneous resonances in σ_1 and σ_2 with two different sets of magnon modes involved. We have plotted the Raman peak shift of the two-magnon line as a function of ω_ℓ in Fig. 3(a), and the corresponding Raman cross-section σ_{xy} (corrected for absorption) vs ω_ℓ in Fig. 3(b). The same results for σ_{xz} are given in Fig. 4.

The results of Figs. 3 and 4 agree well with our earlier description. When $(d\sigma_{\alpha\beta}/d\omega_s)_R > (d\sigma_{\alpha\beta}/d\omega_s)_{NR}$, the Raman shift should obey Eq. (5). We find that we can indeed fit that portion of the data by Eq. (5) assuming $\omega_E(\vec{k})$ is independent of $\vec{k}$. This is shown by the straight lines in Figs. 3(a) and 4(a). The values of constant ω_E deduced from the fit, for RRS near σ_1, σ_2, and π_1 peaks respectively, are $\omega_E(\sigma_1) = 18420.7\ cm^{-1}$, $\omega_E(\sigma_2) = 18429.5\ cm^{-1}$, and $\omega_E(\pi_1) = 18405\ cm^{-1}$. If $\sigma_1(\pi_1)$ and σ_2 are indeed magnon sidebands of e_1 and e_2 and if the assumption of dispersionless $\omega_E(\vec{k})$ is correct, then $\omega_E(\sigma_1)$ and $\omega_E(\pi_1)$ should be equal to the frequency of the e_1 absorption peak and $\omega_E(\sigma_2)$ to the frequency of the e_2 peak. The observed e_1 and e_2 lines are at $\omega_{e1} = 18419.5\ cm^{-1}$ and $\omega_{e2} = 18436.5\ cm^{-1}$.

The agreement between $\omega_E(\sigma_1)$ and ω_{e1} is within the experimental uncertainty, supporting the previous suggestion that the dispersion of the E_1 exciton is less than 0.5 cm^{-1}.[5] There is a discrepancy of 7 cm^{-1} between $\omega_E(\sigma_2)$ and ω_{e2}. This indicates that the E_2 exciton has a negative dispersion of 7 cm^{-1} from the zone center to the zone edge, in agreement with the 6.2 cm^{-1} estimate of Sell et al.[3] The fact that the data can still be fitted by a straight line suggests a negligible dispersion of E_2 near the zone edge. There is a big discrepancy of 14.5 cm^{-1} between $\omega_E(\pi_1)$ and ω_{e1}. Since we know E_1 is nearly dispersionless, this makes us suspect that π_1 is not a magnon sideband of E_1 but of a lower-energy excitonic state. However, no such state has been found in absorption. Similar difficulty exists in the interpretation of the π_1 absorption band.[3] Sell et al.[3] have found that the observed π_1 peak is shifted by about -9 cm^{-1} from the predicted position.

The rest of the data in Figs. 3(a) and 4(a) can be interpreted qualitatively as follows. On the low-energy side of a magnon sideband, when $(d\sigma_{\alpha\beta}/d\omega_s)_{NR}$ becomes more and more dominant over $(d\sigma_{\alpha\beta}/d\omega_s)_R$, the two-magnon line gradually changes into its off-resonance lineshape and the Raman peak shift moves towards the off-resonance value. On the high-energy side close to the peak of a magnon sideband, the resonance enhancement of those two-magnon modes near the zone edge still dominates (consider Eq. (2) with finite damping constants), leaving the peak position of the two-magnon line more or less unchanged.

We have also found that Eq. (4) describes the observed two-magnon resonance Raman enhancement near magnon sidebands quite well. In Figs. 3(b) and 4(b), the theoretical curves are obtained from Eq. (4) using

the experimental lineshape of $(d\sigma_{\alpha\beta}/d\omega_s)_{NR}$ and with $(\sigma_{\alpha\beta})_R$ normalized to its peak value. The discrepancy between theory and experiment is probably a result of the δ-function approximation in the theoretical derivation.

In summary, we have observed two-magnon RRS in MnF_2 around the magnon sidebands. The mechanism for the two-magnon RRS is different from that for the non-resonant case. With a given excitation frequency ω_ℓ, it selects a particular set of two-magnon modes to be most strongly resonantly enhanced. Consequently, because of the presence of magnon dispersion, the two-magnon line shifts in frequency as ω_ℓ varies, and two two-magnon lines show up when simultaneous resonance with two magnon sidebands occurs. The resonance enhancement agrees quite well with a simple theoretical descritpion.

We are indebted to Professor Y. Petroff for his technical help.

This work was supported by the U.S. Energy Research and Development Administration.

REFERENCES

1. See for examples, P. Y. Yu and Y. R. Shen, Phys. Rev. Letters 32, 373, 939 (1974).
2. R. A. Erickson, Phys. Rev. 90, 779 (1953); A. Okazaki and K. C. Turberfield, Phys. Letters 8, 9 (1964).
3. D. D. Sell, R. L. Greene, and R. M. White, Phys. Rev. 158, 489 (1967).
4. R. Loudon, Adv. Physics 17, 243 (1968).
5. R. E. Dietz, A. E. Meixner, H. J. Guggenheim, and A. Misetich, J. Luminescence 1,2, 279 (1970); R. E. Dietz, A. E. Meixner, H. J. Guggenheim, and A. Misetich, Phys. Rev. Letters 21, 1067 (1968).

6. P. A. Fleury, S. P. S. Porto, and R. Loudon, Phys. Rev. Letters 18, 658 (1967).

7. P. A. Fleury and R. Loudon, Phys. Rev. 166, 514 (1968).

8. S. P. S. Porto, P. A. Fleury, and T. C. Damen, Phys. Rev. 154, 522 (1967).

FIGURE CAPTIONS

Fig. 1. Absorption spectrum of MnF_2 at 1.6K between 18400 and 18500 cm^{-1}. The solid and the dashed curves are for polarizations $\perp$ and $\parallel$ to the $\hat{c}$-axis respectively. The inset is a sketch of the relevant energy levels.

Fig. 2. Two-magnon Raman spectra (denoted by M) at several different excitation frequencies ω_ℓ. Peaks I and σ_{1L} correspond to impurity and magnon-assisted luminescence lines respectively.

Fig. 3. (a) Two-magnon Raman shift and (b) Two-magnon Raman cross-section as a function of the excitation frequency ω_ℓ. The exciting and the scattering radiation are polarized along $\hat{y}$ and $\hat{x}$ respectively ($\hat{x},\hat{y} \perp \hat{c}$).

Fig. 4 (a) Two-magnon Raman shift and (b) Two-magnon Raman cross-section as a function of the excitation frequency ω_ℓ. The exciting and the scattering radiations are polarized along $\hat{z}$ and $\hat{x}$ respectively ($\hat{x} \perp \hat{c}$ and $\hat{z} \parallel \hat{c}$).

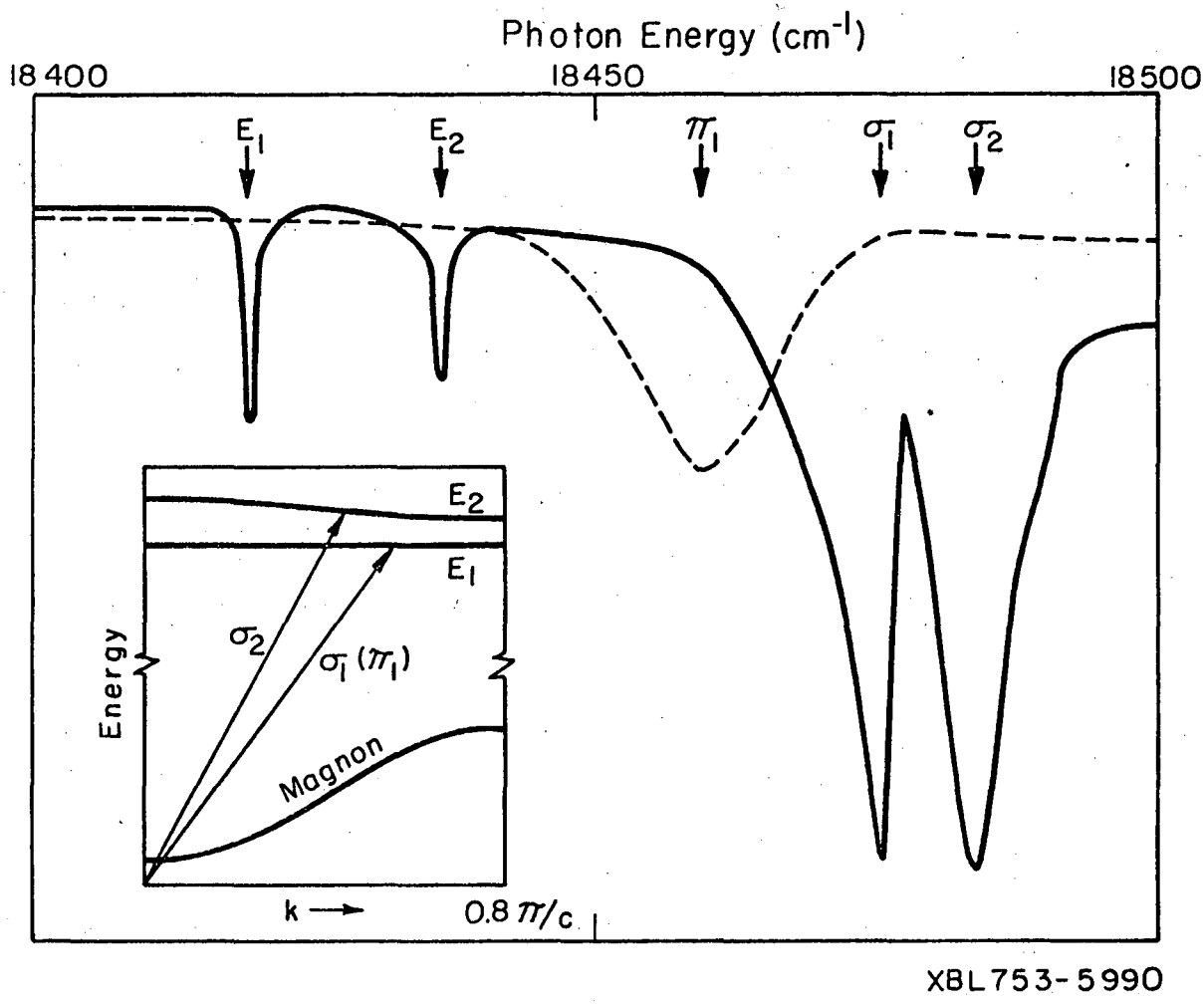

XBL753-5990

Fig. (1)

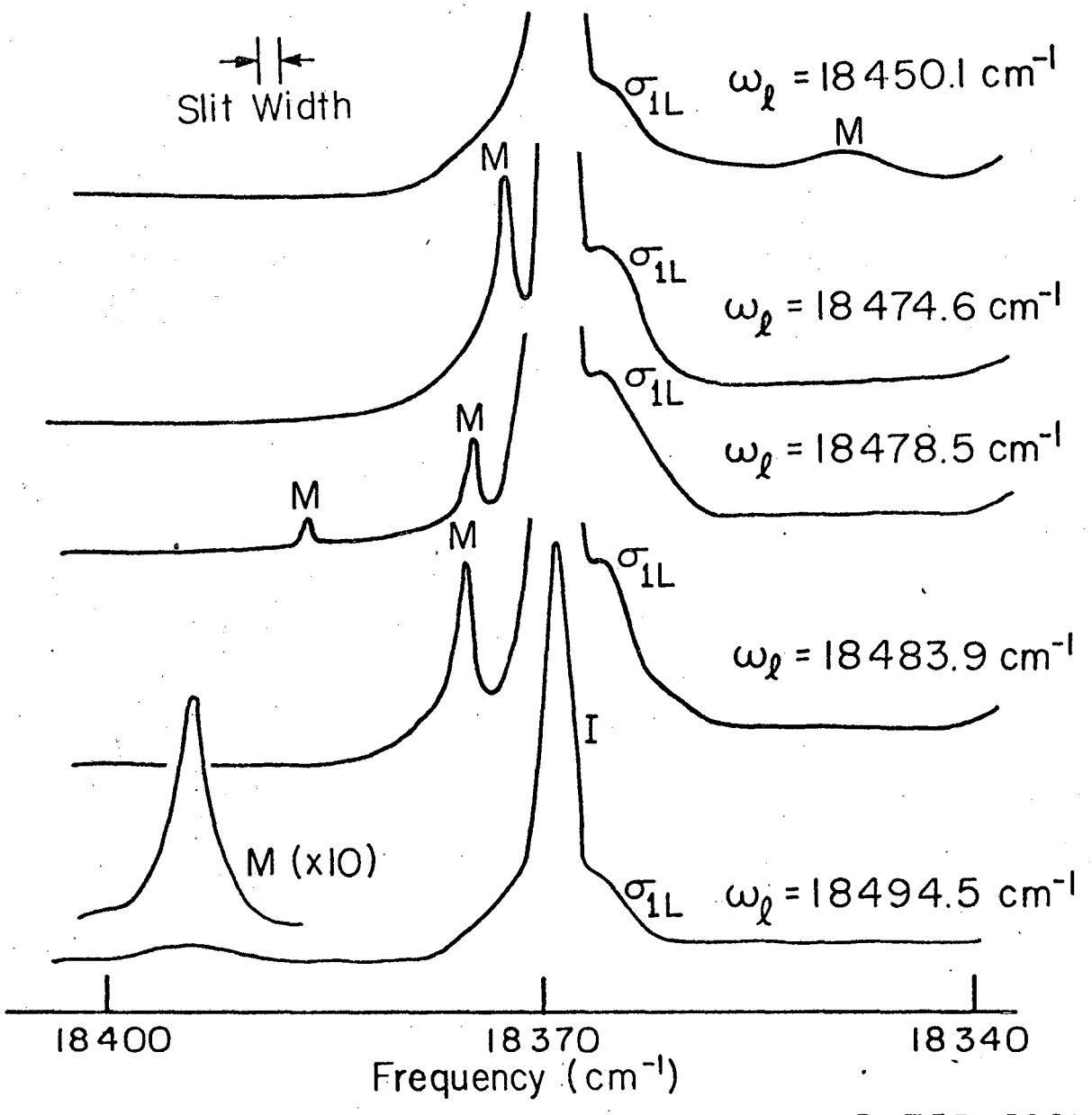

XBL753-5991

Fig. (2)

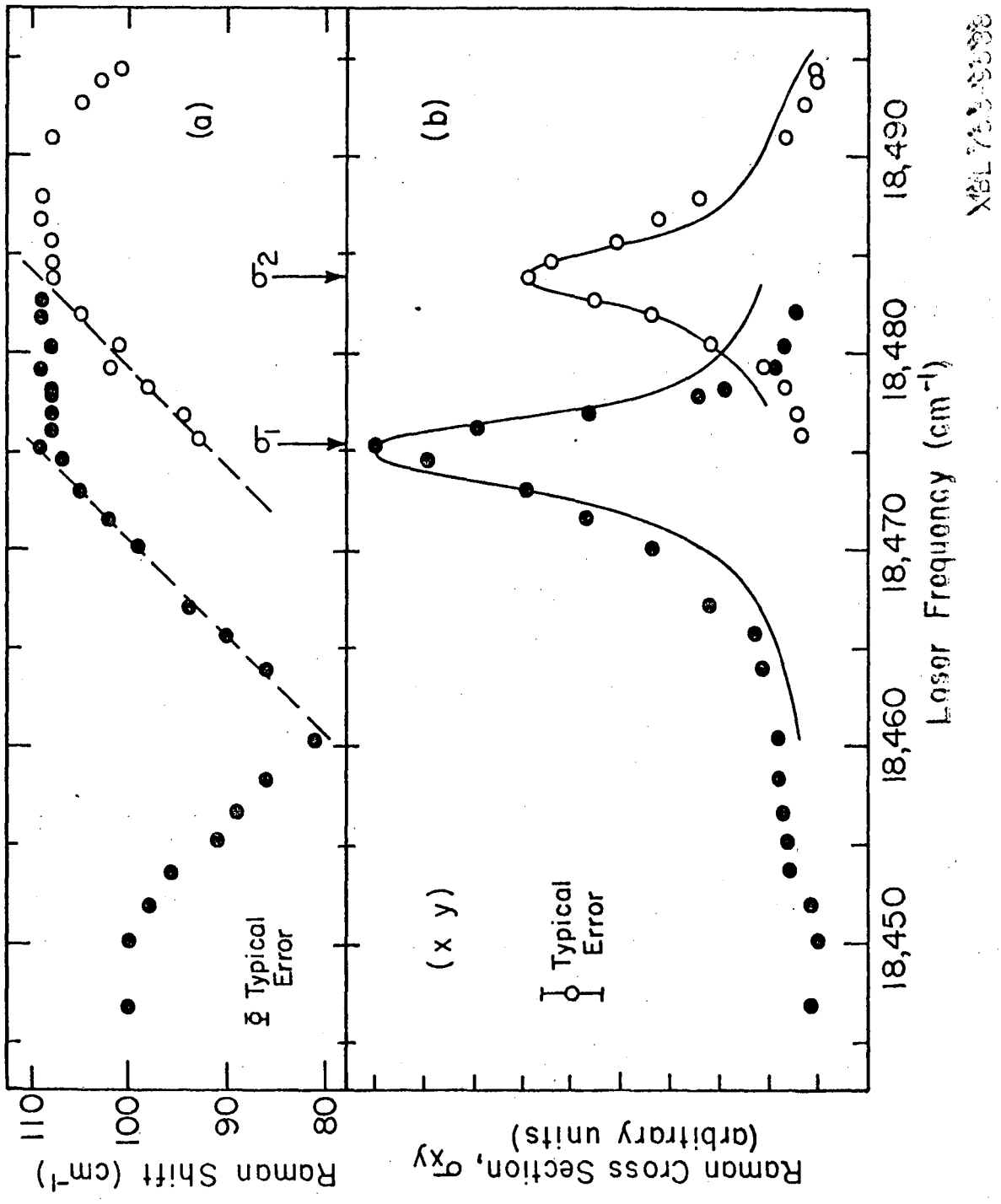

XBL 7[illegible]

Fig. (3)

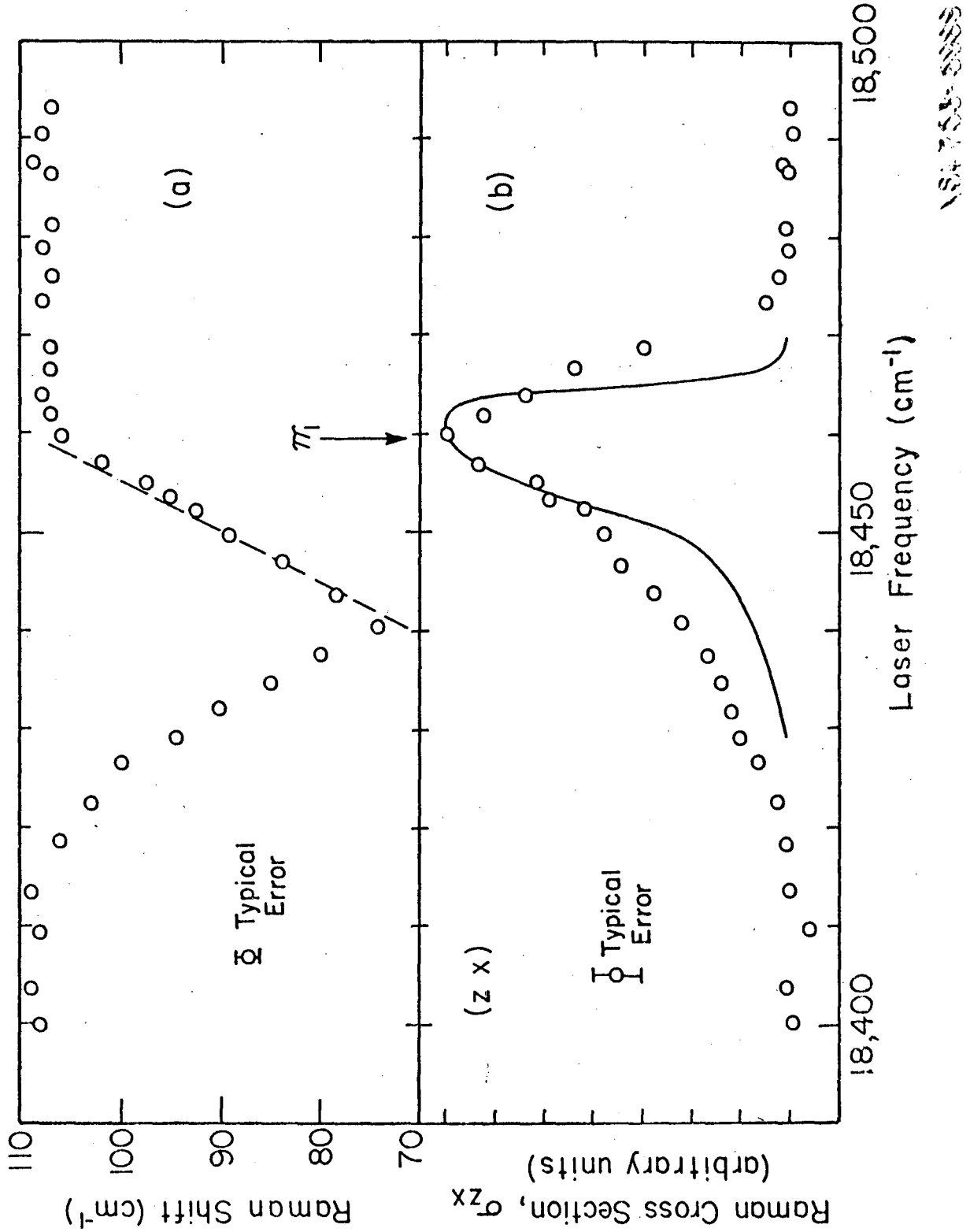
(a)
(b)
π_1
Typical Error
Typical Error
(z x)
Raman Shift (cm^{-1})
Raman Cross Section, σ_{zx} (arbitrary units)
Laser Frequency (cm^{-1})
110
100
90
80
70
18,500
18,450
18,400

Fig. (4)

TECHNICAL INFORMATION DIVISION
LAWRENCE BERKELEY LABORATORY
UNIVERSITY OF CALIFORNIA
BERKELEY, CALIFORNIA 94720